NASA TECHNICAL MEMORANDUM

NASA TM X-64914

SHUTTLE PROPELLANT LOADING INSTRUMENTATION DEVELOPMENT

By John Hamlet
Electronics and Control Laboratory

January 1975

N75-19626
(NASA-TM-X-64914) SHUTTLE PROPELLANT LOADING INSTRUMENTATION DEVELOPMENT (NASA) 33 p HC $3.75 CSCL 14B
Unclas
G3/35 13452

NASA

George C. Marshall Space Flight Center
Marshall Space Flight Center, Alabama

NOTICE

Because of a waiver initiated and signed in compliance with NASA Policy Directive (NPD) 2220.4, para. 5-b, the International System of Units of measurement has not been used in this document.

1. Report No.	2. Government Accession No.	3. Recipient's Catalog No.
NASA TM X-64914		

4. Title and Subtitle	5. Report Date
Shuttle Propellant Loading Instrumentation Development	January 1975
	6. Performing Organization Code

7. Author(s)	8. Performing Organization Report No.
John Hamlet	
	10. Work Unit No.

9. Performing Organization Name and Address	11. Contract or Grant No.
George C. Marshall Space Flight Center Marshall Space Flight Center, Alabama 35812	
	13. Type of Report and Period Covered
12. Sponsoring Agency Name and Address	Technical Memorandum
National Aeronautics and Space Administration Washington, D. C. 20546	14. Sponsoring Agency Code

15. Supplementary Notes

Prepared by Electronics and Control Laboratory, Science and Engineering

16. Abstract

A continuous capacitance sensor was developed and an analog signal conditioner was evaluated to demonstrate the acceptability of these items for use in the Space Shuttle propellant loading system. An existing basic sensor concept was redesigned to provide capability for cryogenic operation, to improve performance, and to minimize production costs. Sensor development verification consisted of evaluation of sensor linearity, cryogenic performance, and stability during vibration. The signal conditioner evaluation consisted mainly of establishing the effects of the variations in temperature and cable parameters and evaluating the stability.

A sensor linearity of 0.04 in. was achieved over most of the sensor length. The sensor instability caused by vibration was 0.04 percent. The cryogenic performance data show a maximum instability of 0.19 percent at liquid hydrogen temperature; and a theoretical calibration can be computed to within 1 percent. The signal conditioner evaluation showed that, with temperature compensation, all error sources typically contribute much less than 1 percent.

An estimate of the accuracy achievable with the sensor and signal conditioner shows an rss estimate of 0.75 in. for liquid oxygen and 1.02 in. for liquid hydrogen. These are approximately four times better than the Shuttle requirements.

Comparison of continuous sensor and discrete sensor performance showed the continuous sensor to be significantly better when there is surface activity due to sloshing, boiling, or other disturbances.

17. Key Words (Suggested by Author(s))	18. Distribution Statement
instrumentation liquid level cryogenic capacitance	Unclassified - Unlimited John D Hamlet

19. Security Classif. (of this report)	20. Security Classif. (of this page)	21. No. of Pages	22. Price
Unclassified	Unclassified	33	NTIS

For sale by National Technical Information Service, Springfield, Virginia 22151

TABLE OF CONTENTS

LIST OF ILLUSTRATIONS

LIST OF TABLES

TECHNICAL MEMORANDUM X- 64914

SHUTTLE PROPELLANT LOADING INSTRUMENTATION DEVELOPMENT

INTRODUCTION

The results of studies to define candidate concepts and components for use in the Shuttle program indicated that, with some development to incorporate certain design changes, existing basic designs for continuous capacitance liquid level instrumentation would offer the most cost-effective approach for the propellant loading system. The performance requirements for the Shuttle loading instrumentation are not as demanding as for previous programs when sophisticated, complex, and costly instrumentation was required; therefore it was surmised that uncompensated sensors and analog type signal conditioners could meet the requirements. To demonstrate this, work was initiated to develop an engineering model sensor and to evaluate existing designs of analog type signal conditioners.

The sensor concept selected for further development was the basic design[1] used in the Saturn program to measure fuel slosh in the S-IC stage. The history of successful use, plus the simple design, introduced a high degree of confidence that the development could be completed successfully.

This report describes the design modifications made to the sensor, the development testing performed to verify the design, and the results of an evaluation of four existing designs of signal conditioners. An accuracy estimate was made to show the expected accuracy of a propellant loading system utilizing the components described in the report.

SENSOR DESCRIPTION

The sensor is shown in Figure 1. The basic parallel plate, open construction of the S-IC fuel slosh, described in NASA TM X-53217, was retained. The modifications consisted of changing all dielectric insulators to Kel-F,

---

1. The basic sensor design is described in NASA TM X-53217, Astronics Research and Development Report No. 3. pp. 72-77.

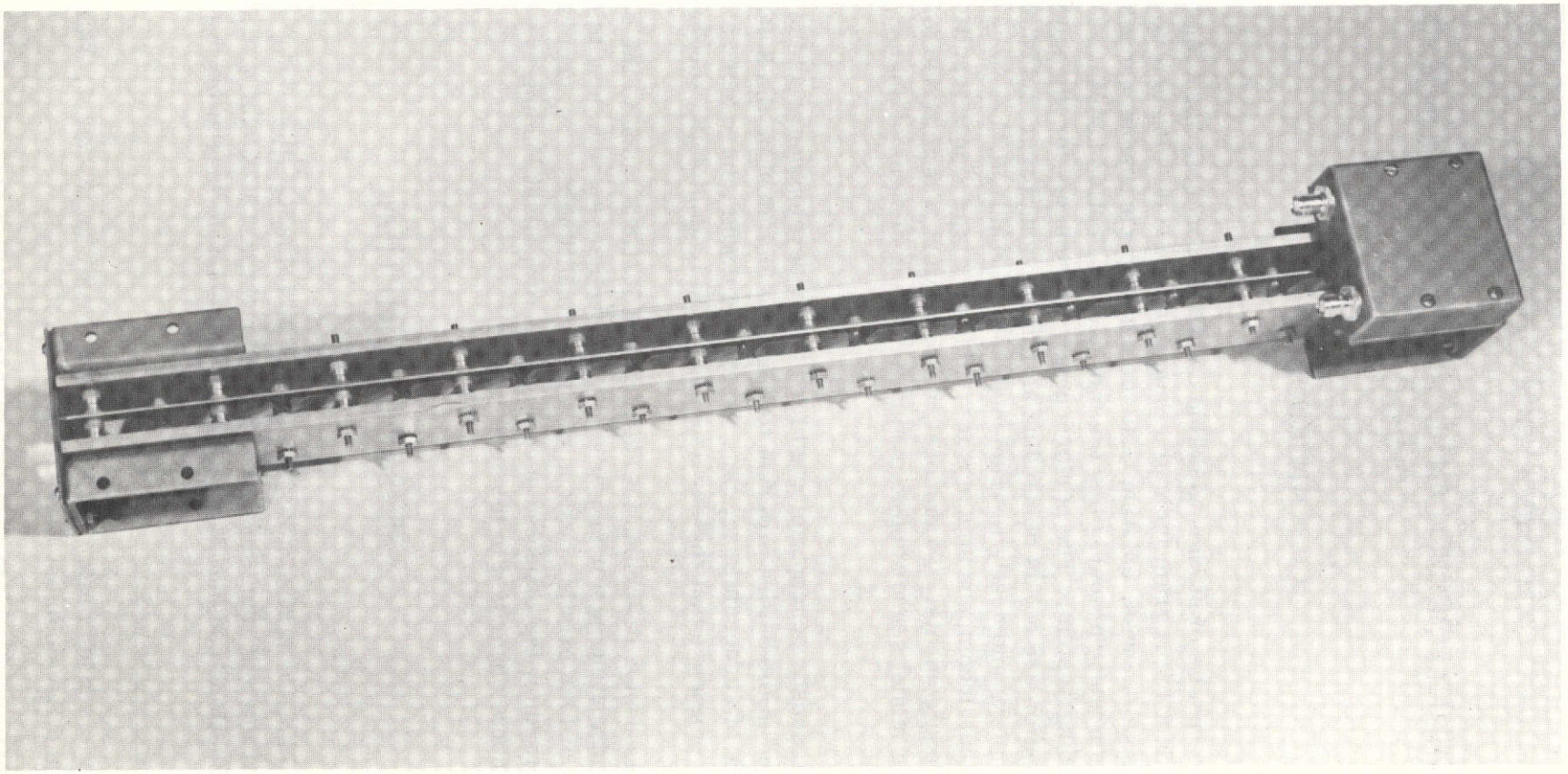

Figure 1. Engineering model sensor.

redesign of the electrode spacers to allow quick assembly of the sensor and to prevent stress buildup during cryogenic operation, redesign of electrodes to improve the linearity, and a redesign of the electrical connectors to eliminate nonstandard parts. The principal features of this type construction are: It allows a rugged construction without complicating the assembly process and without degradation of performance with a low sensor Q; it provides a sensor in which all the capacitance is active, thereby allowing the calibration scale factor to be predicted accurately; it provides an open construction which is less susceptible to contamination; and it provides a fast response. Also the design can be adapted to any length with minimum changes in the basic design.

Cross-sectional views of the sensor and electrode spacers are shown in Figure 2. A grounded guard circuit is provided in each spacer by use of an eyelet which is spring loaded against the stud. The stud in turn is grounded to the sensor guard structure. The configuration of the center electrode is shown in Figure 3. The window cutouts compensate for nonlinearity caused by electrode spacers by reducing the capacitance effect between the spacers by the same amount that the spacers reduce the capacitance.

DESIGN VERIFICATION

Development type testing was used to verify the integrity of the design changes. The tests consisted of linearity, cryogenic performance, and vibration.

Linearity Verification

The linearity of the redesigned electrodes was verified using RP-1 as a test medium. Data were taken in increments of 0.25 in. The deviations for an 8 in. section in the middle of the probe are shown in Figure 4. The maximum nonlinearity is 0.04 in. The fringing of the electrical field causes the nonlinearity to increase to a maximum of 0.2 in. at the end of the sensor. The redesigned electrodes resulted in an improvement in linearity by a factor of two over the original design.

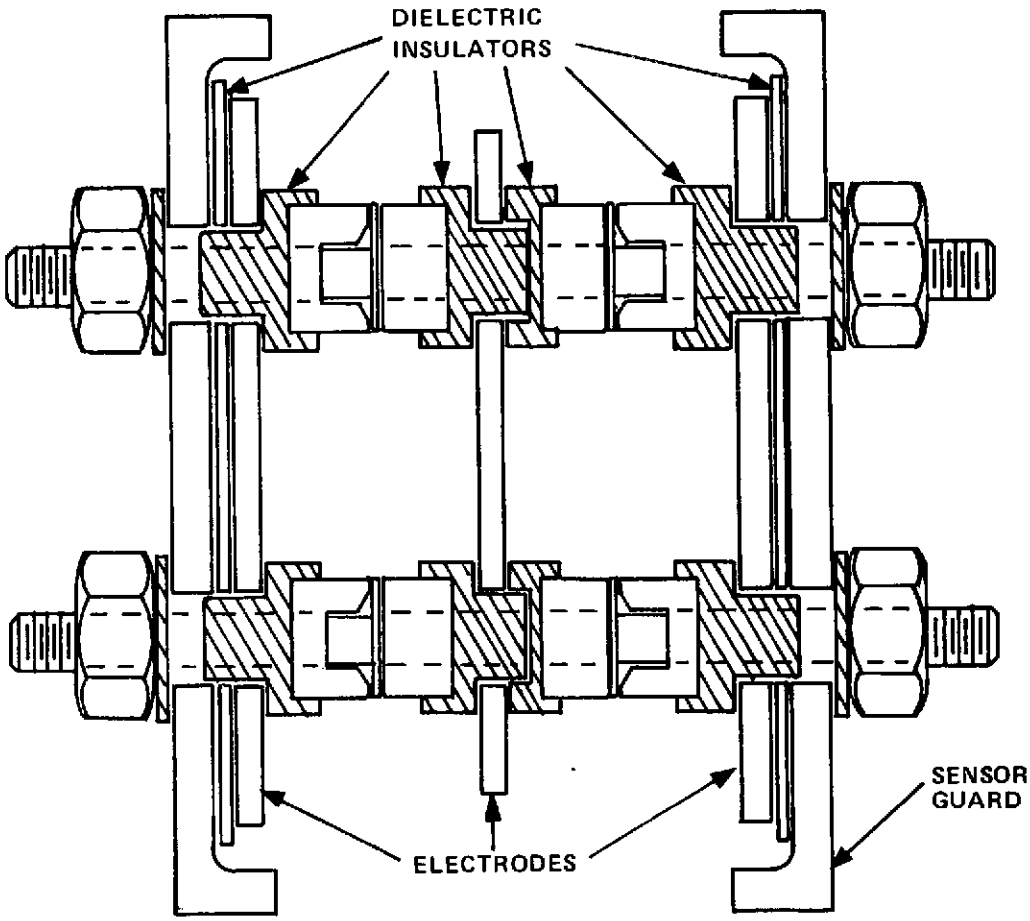

a. Sensor.

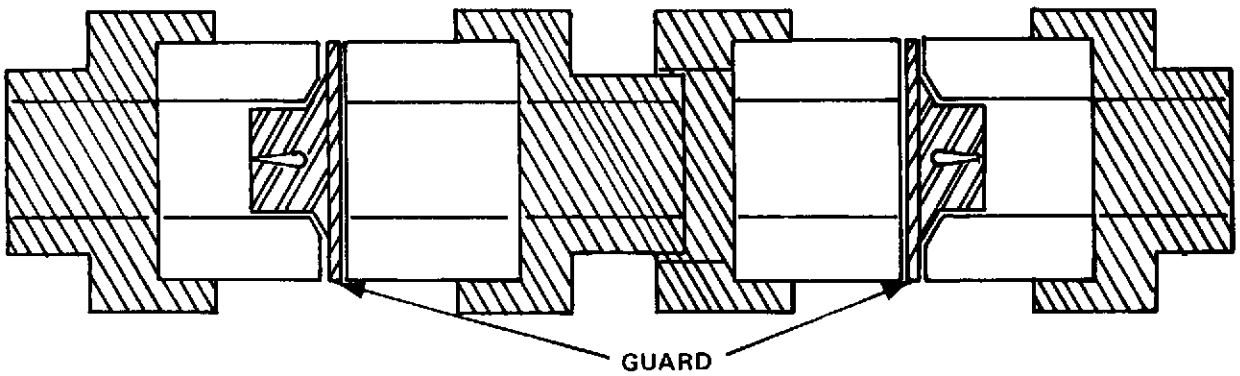

b. Electrode spacers.

Figure 2. Sensor cross section.

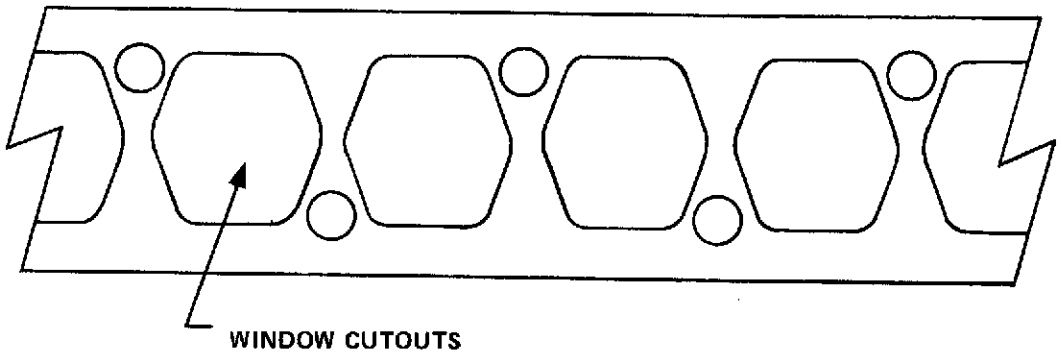

Figure 3. Center electrode configuration.

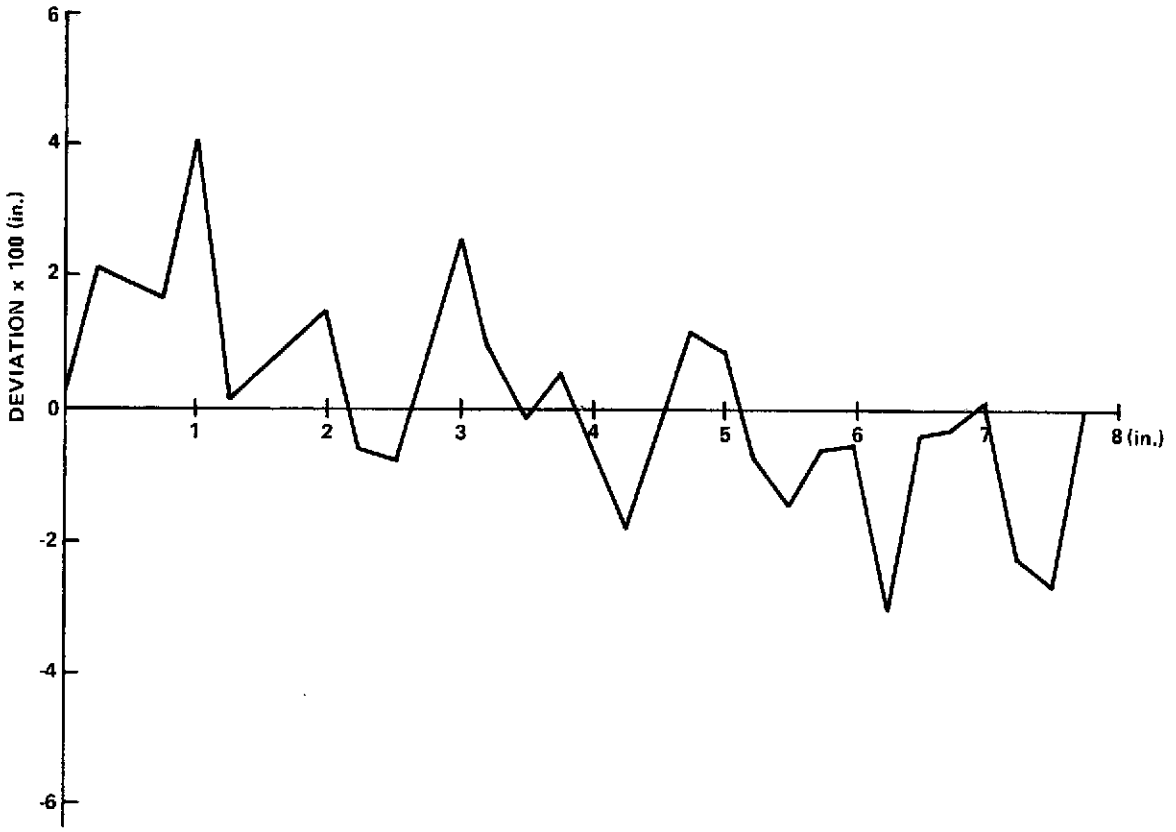

Figure 4. Sensor linearity.

VIBRATION VERIFICATION

Vibration tests were performed to demonstrate the structural integrity and stability of the sensor. Tests were made in three mutually perpendicular axes at two levels, 0.05 g^2/Hz from 20 to 2000 Hz and at 0.2 g^2/Hz from 20 to 2000 Hz.

Measurements of sensor capacitance were made before, during, and after vibration. The maximum change in probe capacitance caused by vibration was 0.009 pF, which is approximately 0.04 percent. The maximum dynamic variation in capacitance during vibration tests was 0.1 pF, which is 0.5 percent. The dynamic variation was symmetrical and, therefore, can be easily filtered out in the signal conditioner.

Cryogenic Performance

Cryogenic evaluation of the sensor was performed to determine the sensor temperature coefficients, to demonstrate stability at cryogenic temperatures, and to determine the accuracy of the theoretical calibration. For these evaluations, point sensors were installed along with the continuous capacitance sensor so that comparative data could be recorded during a typical tank filling operation.

Tests were performed with liquid nitrogen to simulate liquid oxygen, and with liquid hydrogen. The test setups are shown in Figures 5 and 6. The signal conditioner used in these tests was Circuit C. The data were automatically recorded on magnetic tape and strip charts and were manually recorded on a precision capacitance bridge. The results are shown in Tables 1 and 2. The most significant results are summarized at the bottom of each table. The data from tests 4 and 5 are not included because these tests were performed with single conductor shielded wire between sensor and signal conditioner instead of coaxial wire; therefore, the data from these two tests could not be compared with the remaining test data. The probe was modified to incorporate new spacers (from a second source) before liquid hydrogen tests numbers 8 and 9 and liquid nitrogen test number 4 were performed. This accounts for the slightly different sensor capacitances recorded for these tests.

The temperature coefficients seem to be reasonable. The stability at liquid nitrogen temperatures was very good while the stability at liquid hydrogen temperatures was not as good as expected; however, it is acceptable. The

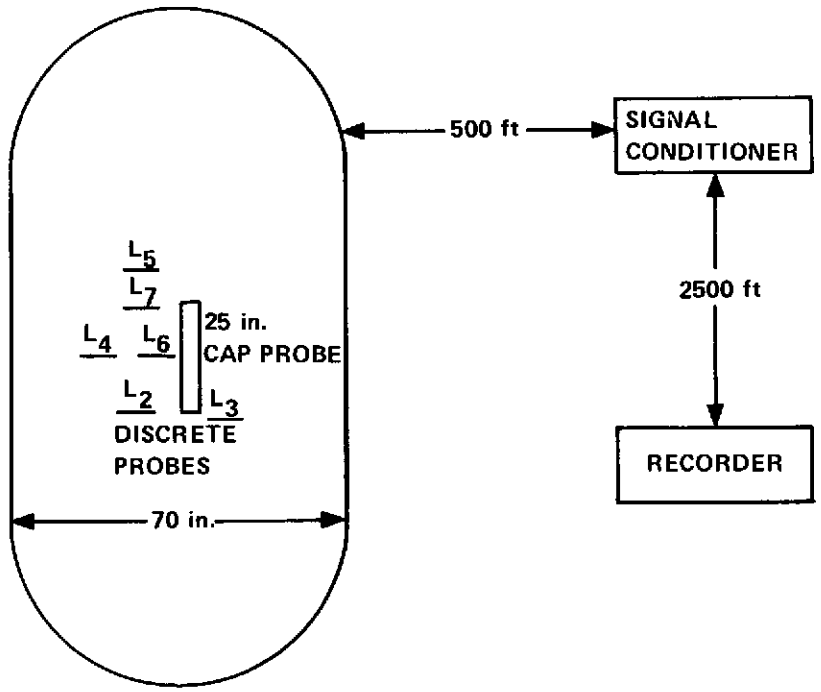

Figure 5. Liquid hydrogen test setup.

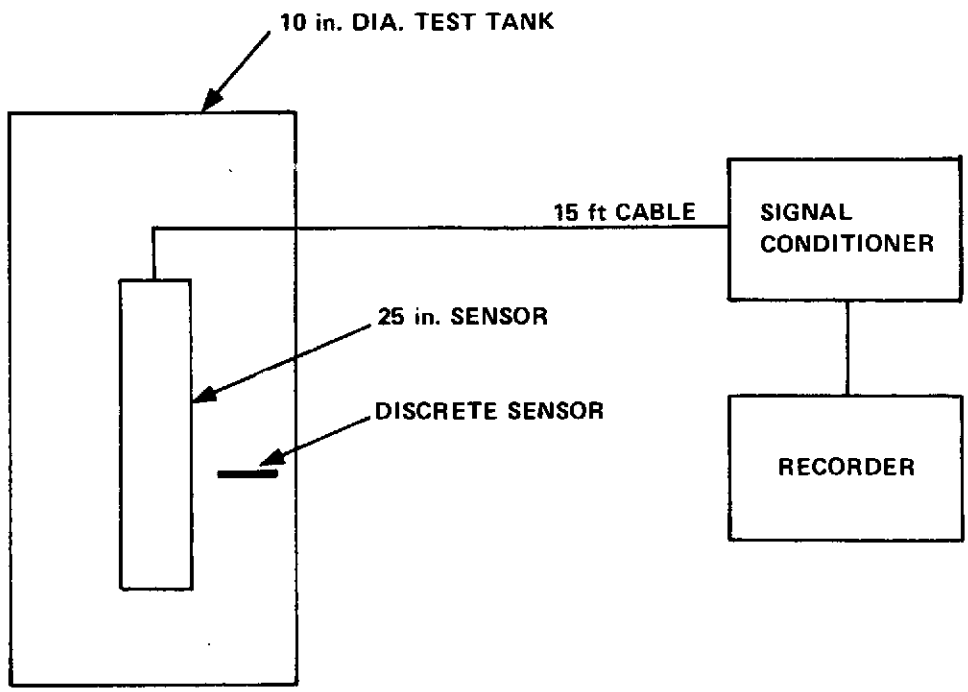

Figure 6. Liquid nitrogen test setup.

TABLE 1. SENSOR PERFORMANCE AT LIQUID HYDROGEN TEMPERATURE

Test No.	Empty Warm Capacitance pF	Warm Vacuum Capacitance[b] pF	Empty Cold Capacitance pF	Cold Vacuum Capacitance pF	Cold Full Capacitance pF	Temp. Coef. (%)	Measured Capacitance Change pF	Predicted Capacitance Change pF	Percent Calibration Difference
1	21.858	21.847	21.720	21.634	26.730	+ 0.97	5.095	5.039	+ 1.09
2	21.810	21.799	21.740	21.654	26.760	+ 0.66	5.105	5.044	+ 1.19
3	21.720	21.709	21.700	21.614	26.730	+ 0.43	5.115	5.035	+ 1.55
6	21.800	21.789	21.760	21.674	26.790	+ 0.53	5.115	5.049	+ 1.29
7	21.810	21.799	21.760	21.675	26.770	+ 0.57	5.094	5.054	+ 0.78
8[a]	21.990	21.979	21.899	21.801	26.889	+ 0.81	5.087	5.074	+ 0.25
9[a]	21.980	21.969	21.891	21.804	26.870	+ 0.75	5.065	5.076	- 0.22

Summary:

Average temperature coefficient = + 0.67%
Average uncertainty in theoretical calibration = + 1.2%
Maximum instability (based on warm vacuum capacitance) = 0.63%
Maximum instability (based on cold vacuum capacitance) = 0.19%

a. Spacers were replaced for these tests.
b. Vacuum capacitances are computed from empty capacitances.

ORIGINAL PAGE IS
OF POOR QUALITY

TABLE 2. SENSOR PERFORMANCE AT LIQUID NITROGEN TEMPERATURE

Test No.	Empty Warm Capacitance pF	Warm Vacuum Capacitance[c] pF	Empty Cold Capacitance pF	Cold Vacuum Capacitance pF	Cold Full Capacitance pF	Temp. Coef. (%)	Measured Capacitance Change pF	Predicted Capacitance Change pF	Percent Calibration Difference
1	21.698	21.686	21.728	21.680	31.14	+ 0.03	9.46	9.40	+ 0.64
2	21.705	21.693	21.723	21.675	31.203	+ 0.08	9.48	9.40	+ 0.85
3	21.705	21.693	21.730	21.682	31.226	+ 0.05	9.54	9.40	+ 1.49
4[a]	22.60[b]	22.59	21.69	21.64	31.12	+ 4.3	9.48	9.38	+ 1.07

Summary:

Average temperature coefficient (excluding Test No. 4) = + 0.05%
Average uncertainty in theoretical calibration = 1.0%
Maximum instibility (based on warm vacuum capacitance) = 0.03%
Maximum instability (based on cold vacuum capacitance) = 0.03%

a. Spacers were replaced for this test.
b. Data point not reliable.
c. Vacuum capacitances are computed from empty capacitances.

ORIGINAL PAGE IS OF POOR QUALITY

1 percent average uncertainty in the theoretical calibration is attributed to uncertainties in the liquid dielectric constant. Most of this error can be eliminated by individual sensor calibration. Since a continuous sensor provides a measurement of instantaneous liquid level , it is expected that a measurement of average liquid level, which is desirable for tanking, could be obtained by integrating and averaging the output as follows:

$$\text{Average Liquid Level} = \frac{\int_0^T \text{sensor output dt}}{T} .$$

Figures 7 and 8 show playback of data recorded during the liquid hydrogen tests. The data were played back through various filters which provided an approximation to the above equation. Filters were applied to the discrete sensor outputs to provide a measurement of duty cycles. Figure 7(a) shows the unfiltered data from the 25 in. continuous sensor while 7(b) shows that, when the same data are passed through a low pass filter, an output proportional to average liquid level is obtained. The velocity lag caused by this filter was 0.8 in. The peak-to-peak surface noise is approximately 6 in. Figures 7(c) through 7(f) show unfiltered and filtered data from two discrete sensors installed at the center of the continuous sensor. The discrete sensors cycle wet and dry over a liquid level range of 5.6 in. This would be expected from the 6 in. slosh noted from the continuous probe measurement. The variation between the outputs of the two discrete sensors is very small (less than 0.25 in.) around the 50 percent duty cycle point. Also the 50 percent duty cycle point appears to be an accurate representation of the actual liquid level obtained from the continuous sensor. Figure 8 shows data from the continuous sensor and data from one discrete sensor played back through different filters. During this test the test tank was filled to approximately 12 in. on the 25 in. sensor. Then it was pressurized and vented to achieve different levels of surface activity. A comparison of the filtered discrete sensor data shows that the output, even at the 50 percent duty cycle point, will depend on the filter characteristics. The data also show discrete sensor nonrepeatability of up to 3 in. when used where the surface wave activity is not constant. These test results are consistent with the expected results of analysis of the discrete sensor characteristics, as shown in Appendix A.

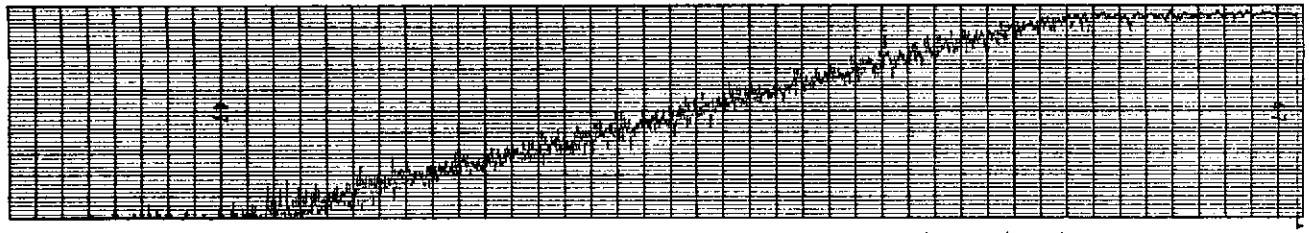

a. Measurement L_3, time constant = 0 (8 sec/div.)

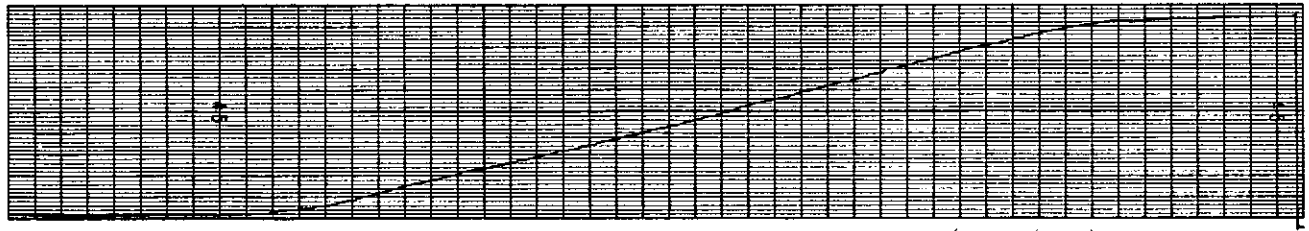

b. Measurement L_3, time constant = 10 sec (8 sec/div.)

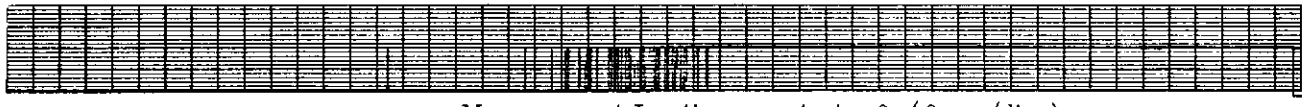

c. Measurement L_6, time constant = 0 (8 sec/div.)

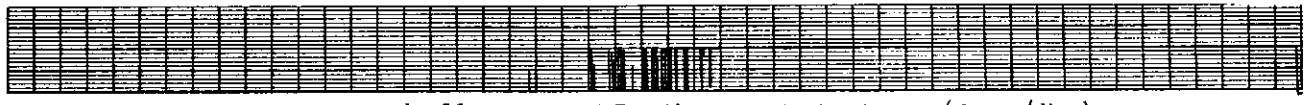

d. Measurement L_4, time constant = 0 sec (8 sec/div.)

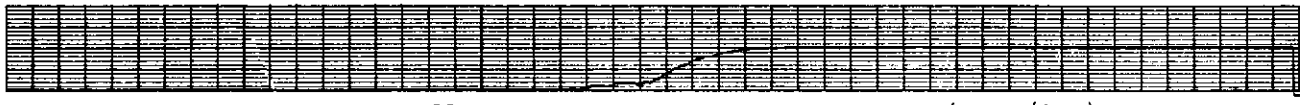

e. Measurement L_6, time constant = 20 sec (8 sec/div.)

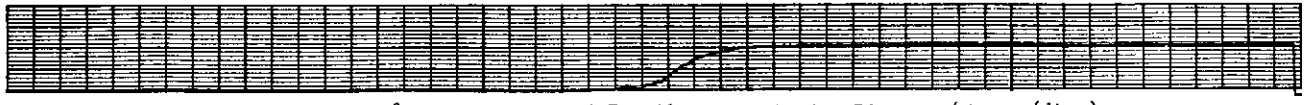

f. Measurement L_4, time constant = 20 sec (8 sec/div.)

Figure 7. Liquid hydrogen test data.

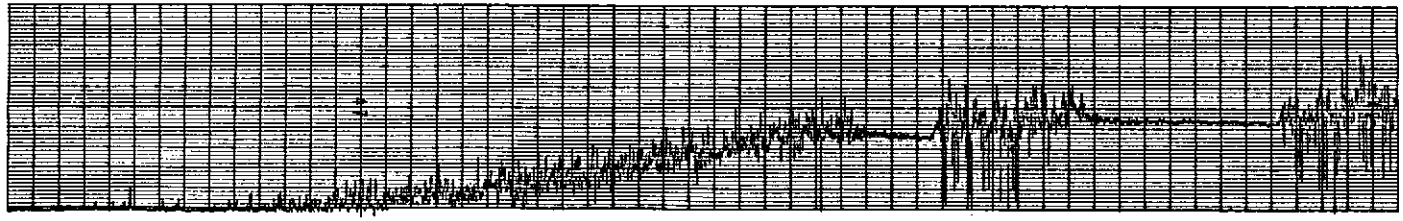

a. Measurement L_3, time constant = 0 (8 sec/div.)

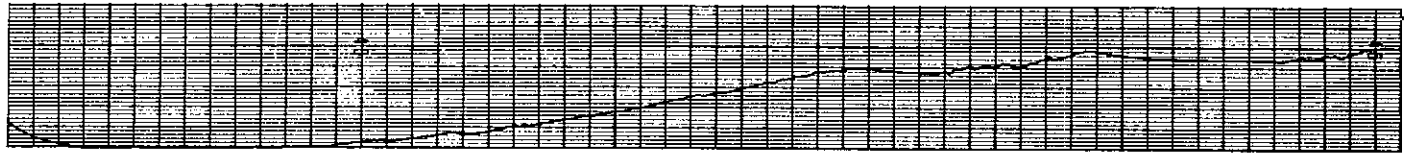

b. Measurement L_3, time constant = 10 sec (8 sec/div.)

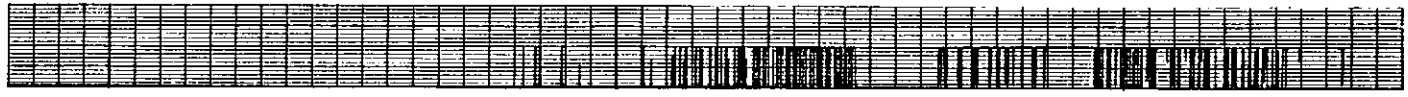

c. Measurement L_6, time constant = 0 (8 sec/div.)

d. Measurement L_6, time constant = 5 sec (8 sec/div.)

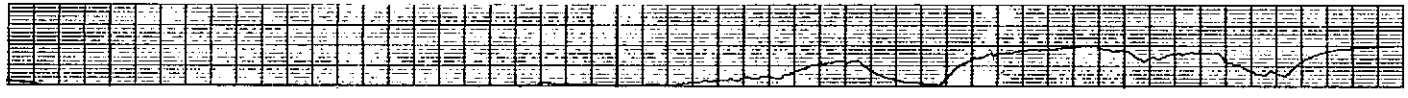

e. Measurement L_6, time constant = 10 sec (8 sec/div.)

f. Measurement L_6, time constant = 20 sec (8 sec/div.)

Figure 8. Liquid hydrogen test data.

SIGNAL CONDITIONER EVALUATION

Low cost analog type signal conditioning equipment was evaluated to determine the feasibility of using existing basic designs with the sensor and to identify desirable design changes. Four different designs were evaluated. The following is a brief description of the four signal conditioners:

1. Circuit A — The block diagram for Circuit A is shown in Figure 9. This equipment has a history of successful use in commercial applications. The main features are a stabilized excitation oscillator, capability for dielectric compensation, and capability for self-calibration. The operating range of the equipment as delivered was 150 to 190 pF.

2. Circuit B — The Circuit B block diagram is shown in Figure 10. This basic design has a history of successful use in commercial and military applications. The main features are a stabilized amplifier achieved by use of capacitance feedback, and simple alignment requirements. The operating range of the circuit as delivered was 150 to 185 pF.

3. Circuit C — The block diagram for Circuit C is shown in Figure 11. This equipment has a history of successful use in support of aerospace projects. The main features are a stabilized excitation oscillator and capability of driving long cables.

4. Circuit D — The block diagram for Circuit D is shown in Figure 12. This equipment is in the final development phase and operation has been demonstrated in field type installations. The main feature of this circuit is automatic null balance of both signal and quadrature components of the sensor output.

Evaluation of the signal conditioners consisted of temperature tests, determination of the effects of cable variations, and stability tests. For comparison, all of the signal conditioners were set up to operate over a range of 70 to 86 pF since this is the range anticipated to be required for the Shuttle hydrogen tank. Evaluation was made by simulating the hydrogen sensor since this would represent the worst case for the signal conditioners. Since Circuit A and Circuit B were modified by NASA to change the range, tests were made on these before modification to establish the performance of the units as delivered by the vendor.

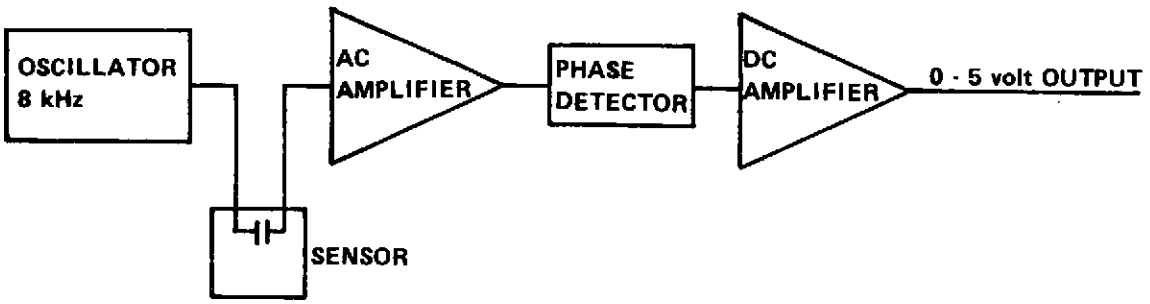

Figure 9. Circuit A.

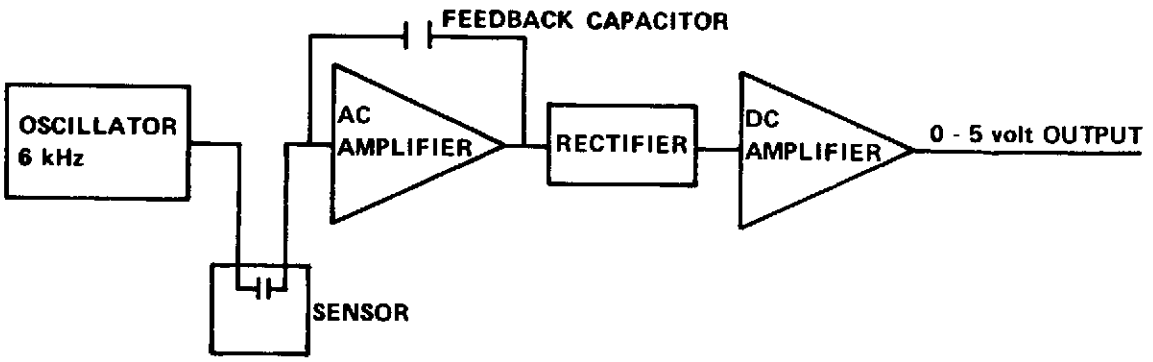

Figure 10. Circuit B.

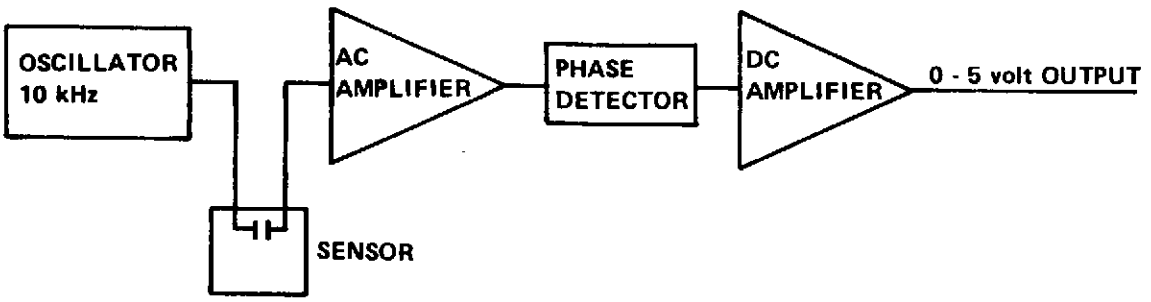

Figure 11. Circuit C.

The setup for the evaluation is shown in Figure 13. The sensor was simulated by the three capacitors as shown in the figure. Temperature tests were performed to the limits of +70° C to -20° C. The effects of cable length variations were established by varying the cable length by 7.5 percent. Additional considerations in using long cables between sensor and signal conditioner were noted in liquid hydrogen tests of the sensor and are discussed in Appendix B. The stability was established by monitoring the output of the signal conditioner, every minute, over a 24 hour period. The repeatability was determined from three calibrations, at ambient temperatures, performed during temperature testing. A summary of the evaluation results is shown in Table 3. Figures 14 through 17 show performance data for each signal conditioner.

It appears that the circuit modification performed by NASA to change the range of Circuits A and B caused some abnormal performance which would not be expected had the circuits been manufactured and tested to the desired range by the vendors. The numbers in parentheses in Table 3 show the performance of Circuits A and B before modifications where there is significant difference. It is expected that these performance figures are more representative of what could be expected from Circuits A and B. The 8.2 percent temperature error for Circuit A occurs at -20° C and is only 3 percent down to -15° C. Circuit A also shows less temperature error when operated with less shunt capacitance simulated at the sensor. It is expected that a repackage of Circuit A would improve the repeatability and stability since the equipment was delivered in an open rack installation. There should be no problem in achieving a linearity of much better than 1 percent for Circuit B with minor design modifications.

It is concluded from the evaluation that it is feasible to achieve an overall accuracy of 1 percent with any of the signal conditioners after appropriate design changes. The major source of error in all circuits is temperature errors. Temperature compensation was not incorporated in Circuits A, C, and D, and it is expected that minor design changes can reduce the temperature errors to an acceptable level.

The design changes required to provide a signal conditioner adequate for use in the Shuttle program are listed in Table 4. All of the desired changes are considered minor and routine.

ACCURACY ESTIMATE

An estimate of the accuracy of the capacitance loading instrumentation was made and is shown in Table 5. The estimates incorporate values established during development of the sensor. Sensor stability was determined by testing.

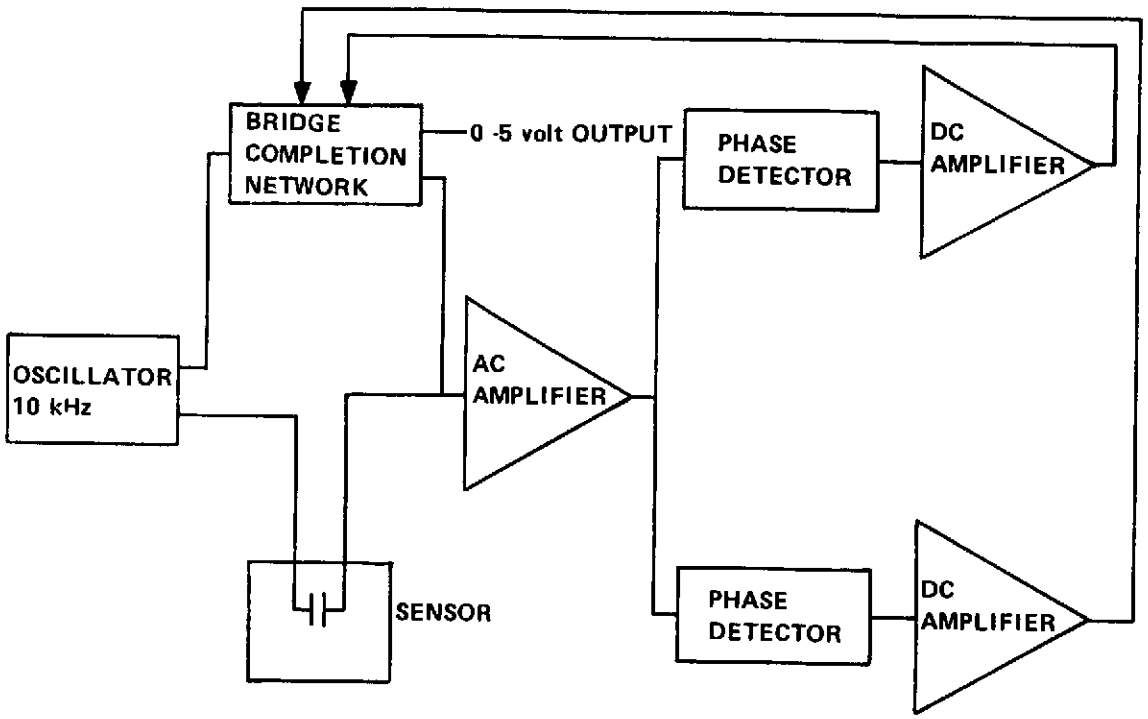

Figure 12. Circuit D.

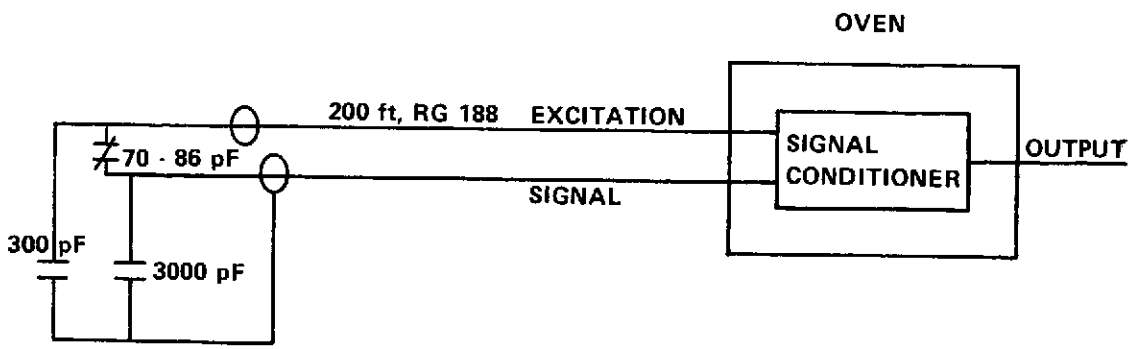

Figure 13. Test setup for signal conditioner evaluation.

TABLE 3. SUMMARY OF SIGNAL CONDITIONER EVALUATION

(all figures are percent of full scale)[a]

Parameter	Circuit A	Circuit B	Circuit C	Circuit D
Nonlinearity	0.03	6.5 (0.65)	0.30	2.5
Temperature Error	8.2 (2.3)	0.64 (0.81)	3.3	2.2
Repeatability	1.5 (1.0)	0.35	1.7	0.94
Cable Length Variation	0.16	0.30	0.31	0.24
Stability	0.70	0.52	0.26	0.32

a. Numbers in parentheses are performance before modification for those cases where there was a significant difference noted during testing.

Effects of liquid and gas density uncertainties are based on a saturated condition over tank pressure ranges caused by atmospheric pressure variation and pressure drop across the vent valves. Errors due to wave action is negligible because integration and averaging can be used. Thermal contraction errors assume a 10 percent uncertainty in the dimensional temperature coefficient of the sensor. The effects of bubbles are as predicted for the S-II loading instrumentation. The calibration error is based on individual calibration for each sensor. The error due to cable parameters was determined by testing.

The electronics error estimate is based on the evaluation of the signal conditioners. No major problem areas were discovered; therefore, it is estimated that a 1 percent total error band for the electronics is readily achievable.

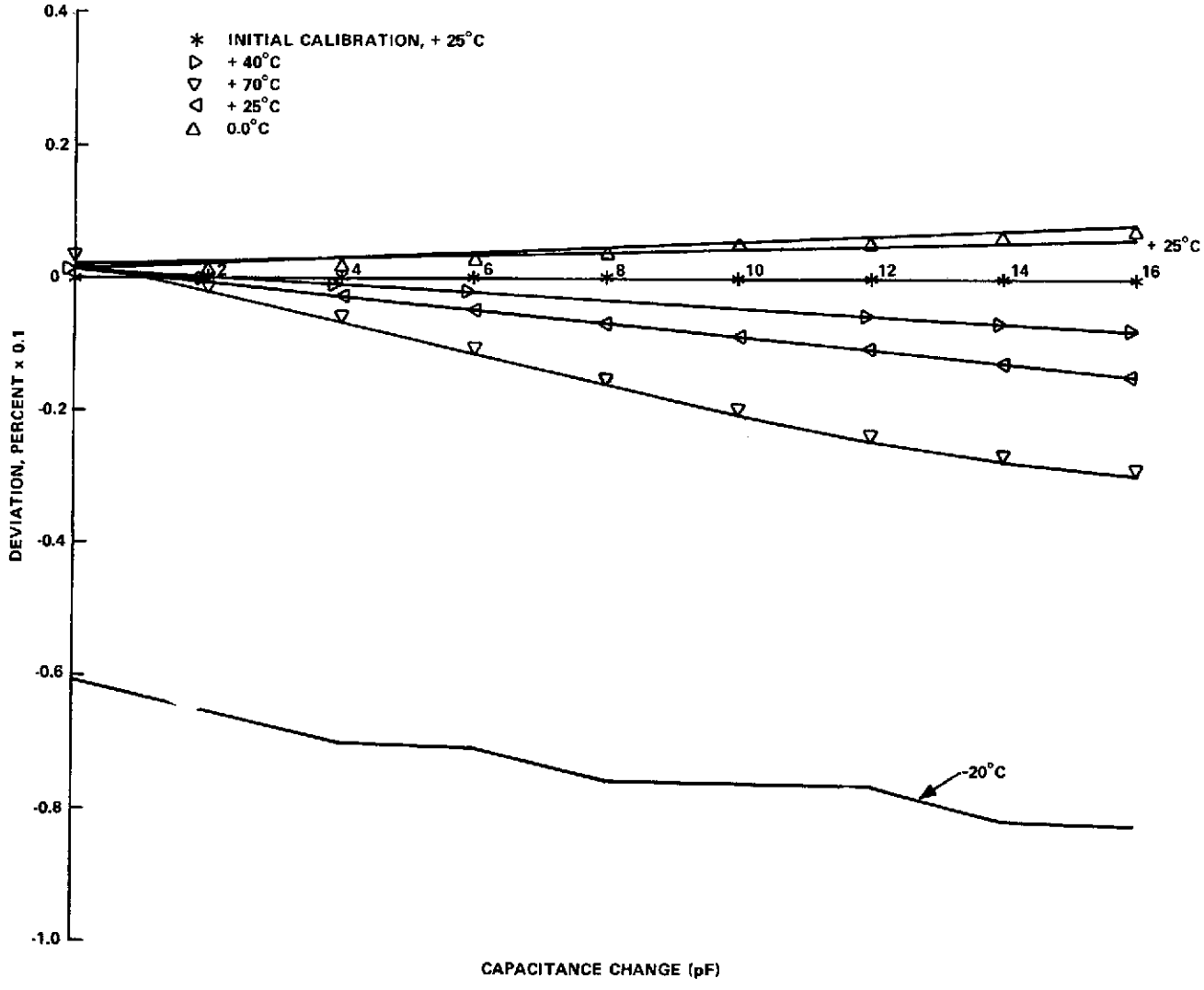

Figure 14. Performance data Circuit A.

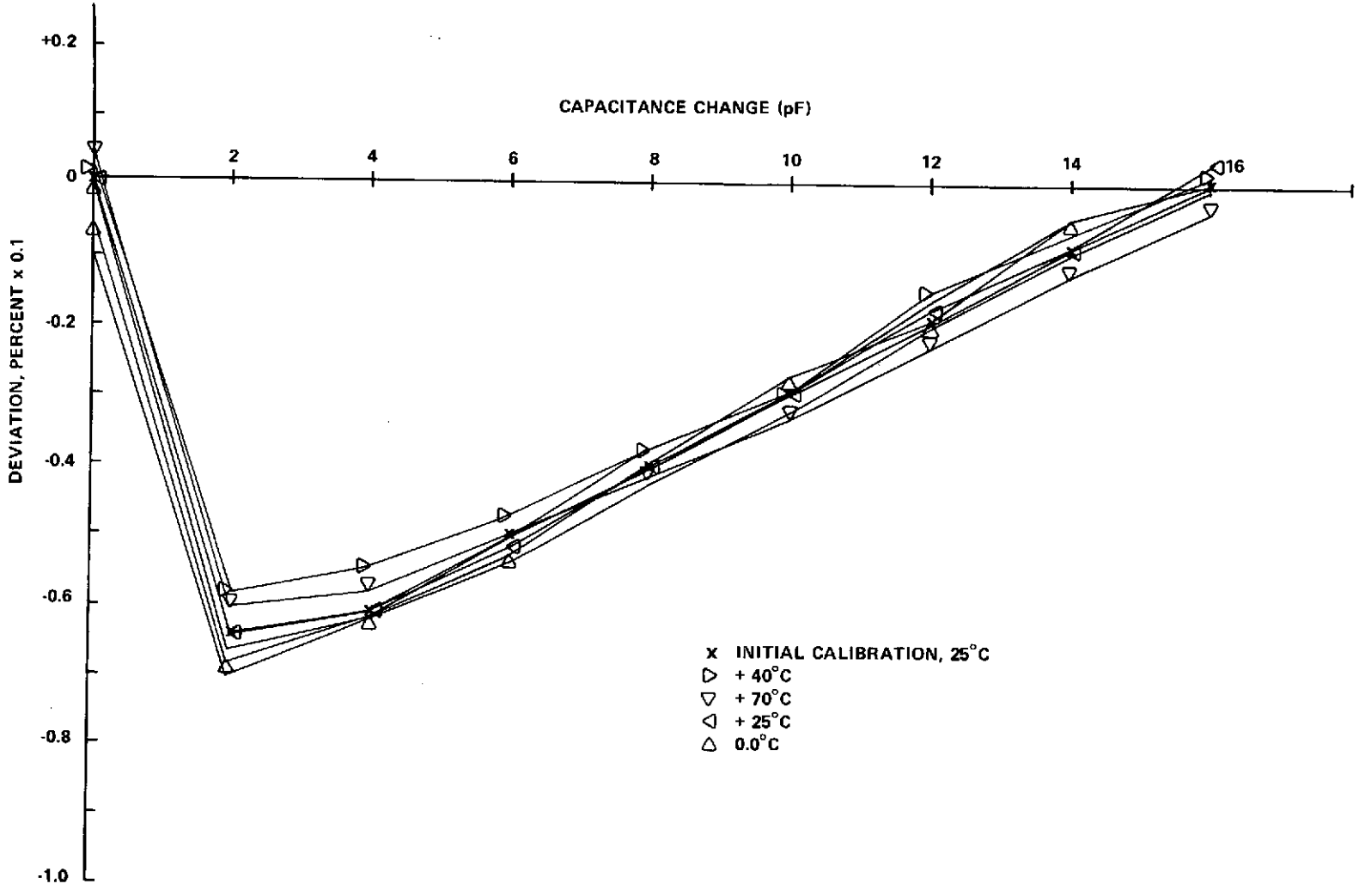

Figure 15. Performance data Circuit B.

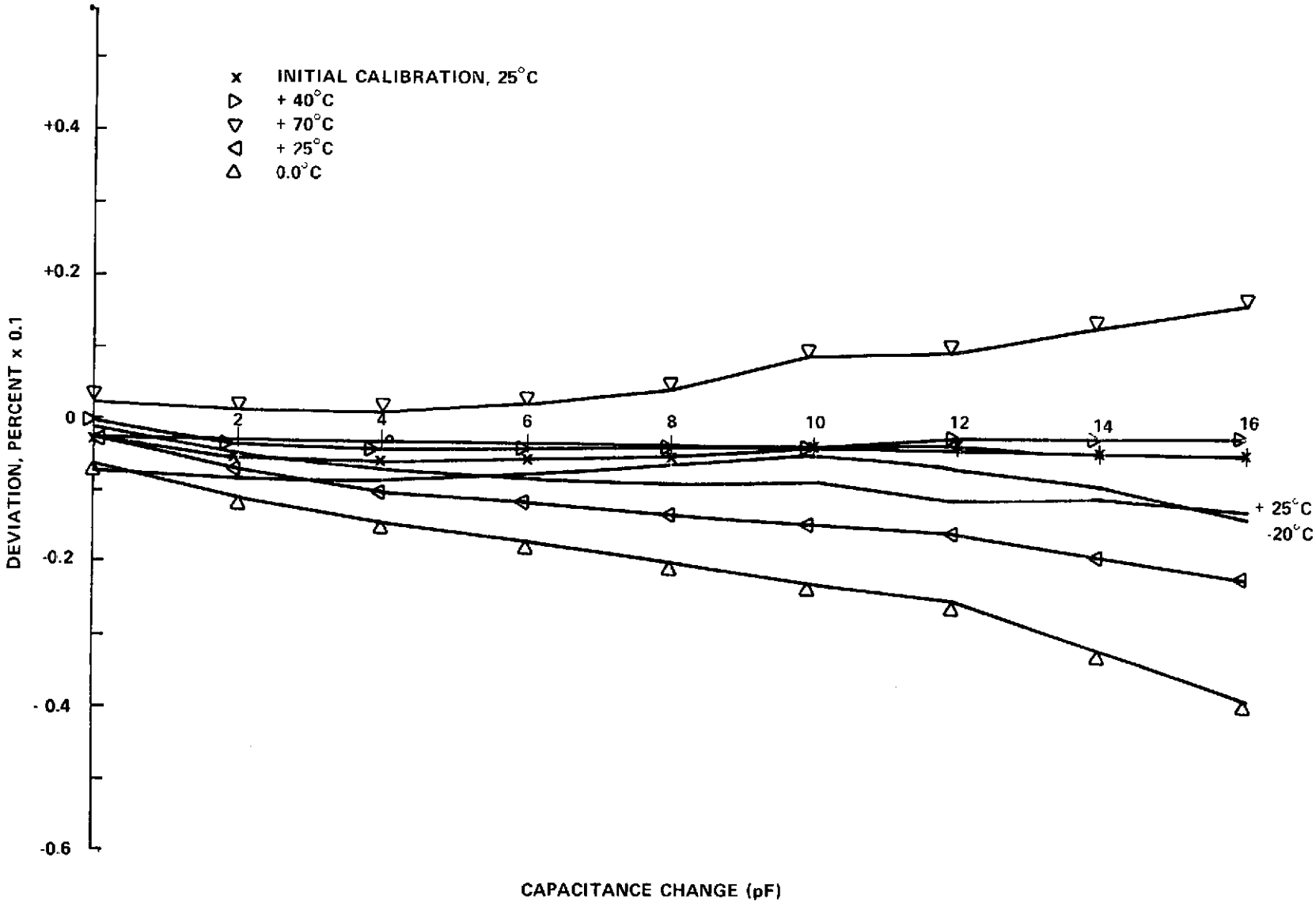

Figure 16. Performance data Circuit C.

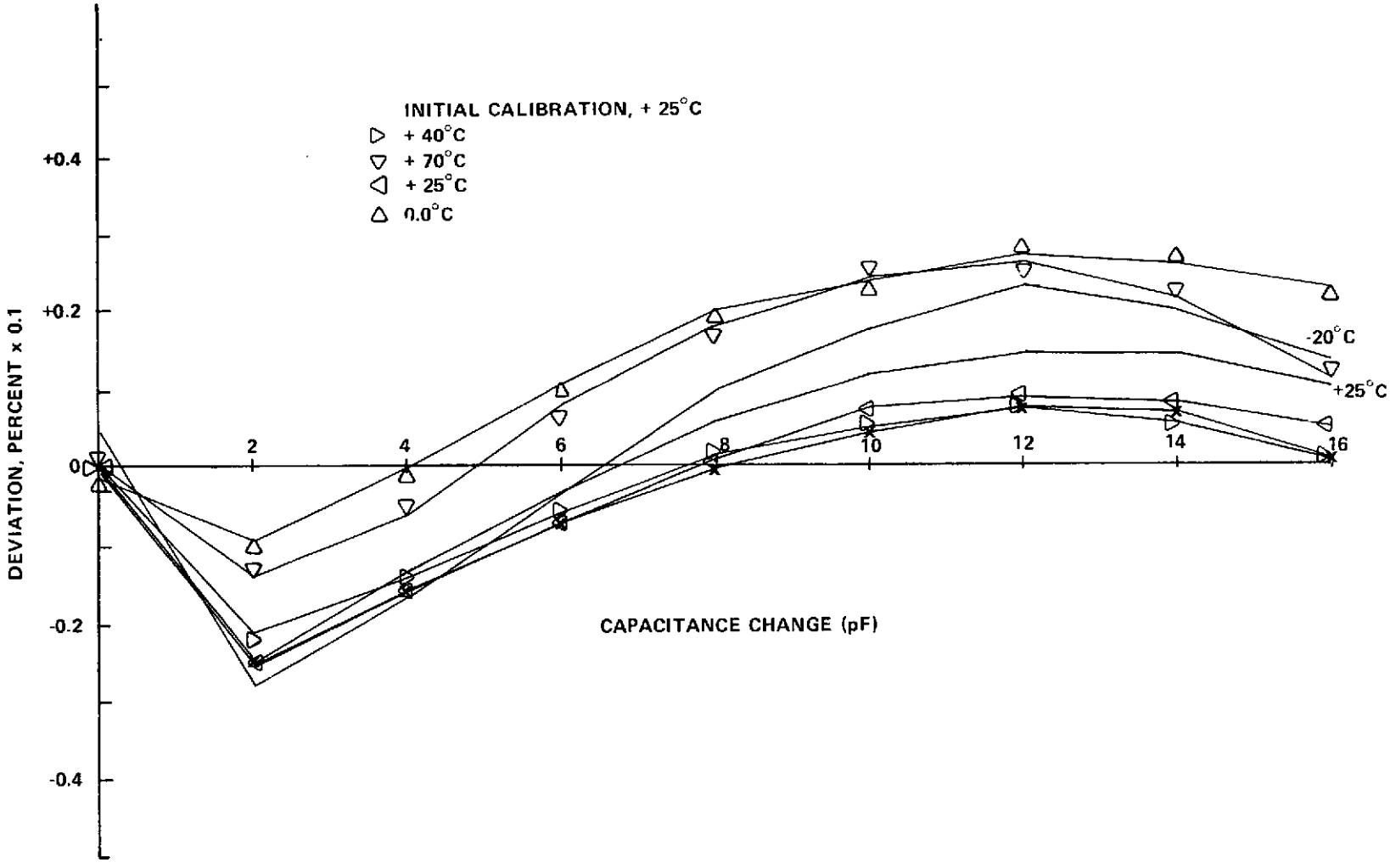

Figure 17. Performance data Circuit D.

TABLE 4. RECOMMENDED DESIGN CHANGES

	Circuit A	Circuit B	Circuit C	Circuit D
Temperature Compensation	X		X	X
Power Converter and Output Isolation	X	X	X	X
Quadrature Adjust Capability		X		
RFI Filters	X	X	X	X
Simplify Alignment Capability	X			
Repackaging	X	X	X	X

TABLE 5. ERROR ESTIMATE FOR 70 in. CAPACITANCE PROPELLANT LOADING INSTRUMENTATION

	LOX Error (in.)	LH_2 Error (in.)
Sensor Stability (0.19%)[a]	0.04	0.56
Liquid Density Uncertainty[a]	0.17	0.31
Wave Action	0.00	0.00
Gas Density Uncertainty[a]	0.01	0.08
Thermal Contraction[a]	0.03	0.03
Bubble Effects[a]	0.17	0.32
Calibration Error	0.04	0.04
Cable Parameters[a]	0.11	0.21
Sensor RSS	0.27	0.75
Electronics Error[a]	0.70	0.70
RSS	0.75	1.02

a. These are percentage errors; others are fixed inches.

APPENDIX A. USE OF DISCRETE SENSORS FOR PROPELLANT LOADING

Discrete liquid level sensors have been proven to be highly accurate when used in applications where the liquid surface is relatively static, that is, no sloshing or surface activity due to boiling or other disturbances. If similar accuracies could be achieved in propellant tanking applications the discrete sensor would be considered a candidate for these applications. During a typical cryogenic tanking operation the propellant surface is disturbed because the propellants are boiling and there is sloshing due to wind disturbances, etc; therefore, as the liquid level approaches a discrete sensor, the sensor output will cycle wet and dry over a liquid level range depending on the amount of surface activity. Typical operation is shown in Figure 7.

Since the discrete sensor does not provide an instantaneous measurement of liquid level, integration and averaging techniques used with continuous sensors could not be expected to be useable except under certain limited conditions. Therefore, an analysis was performed to establish these limitations. It has been proposed to use the duty cycle (percent of time the sensor is wet) of the sensor as a measurement of the liquid level when the sensor is cycling wet and dry. This type output was assumed for the analysis. Also a simple first order slosh was assumed at a frequency well below the fundamental resonant frequency of the tank, and the tanking rate was slow compared to the slosh period. This would represent the best case for the discrete sensor and would define the highest accuracy achievable.

Figure A-1 shows the results of the analysis for different levels of surface activity. These plots agree with the test data of Figures 7 and 8 except that the curvature is reversed. This reversal is probably caused by the test data surface disturbances containing some higher harmonics of the slosh frequency and also by the filters used in the data reduction.

The following conclusions can be drawn from the analyses, which are in agreement with the experimental results:

1. The 50 percent duty cycle point is an accurate measurement of the average liquid level under simple slosh conditions at slow fill rates.

2. The use of the total duty cycle range, 0 to 100 percent, as an accurate measurement requires knowledge of the amplitude of the surface disturbances.

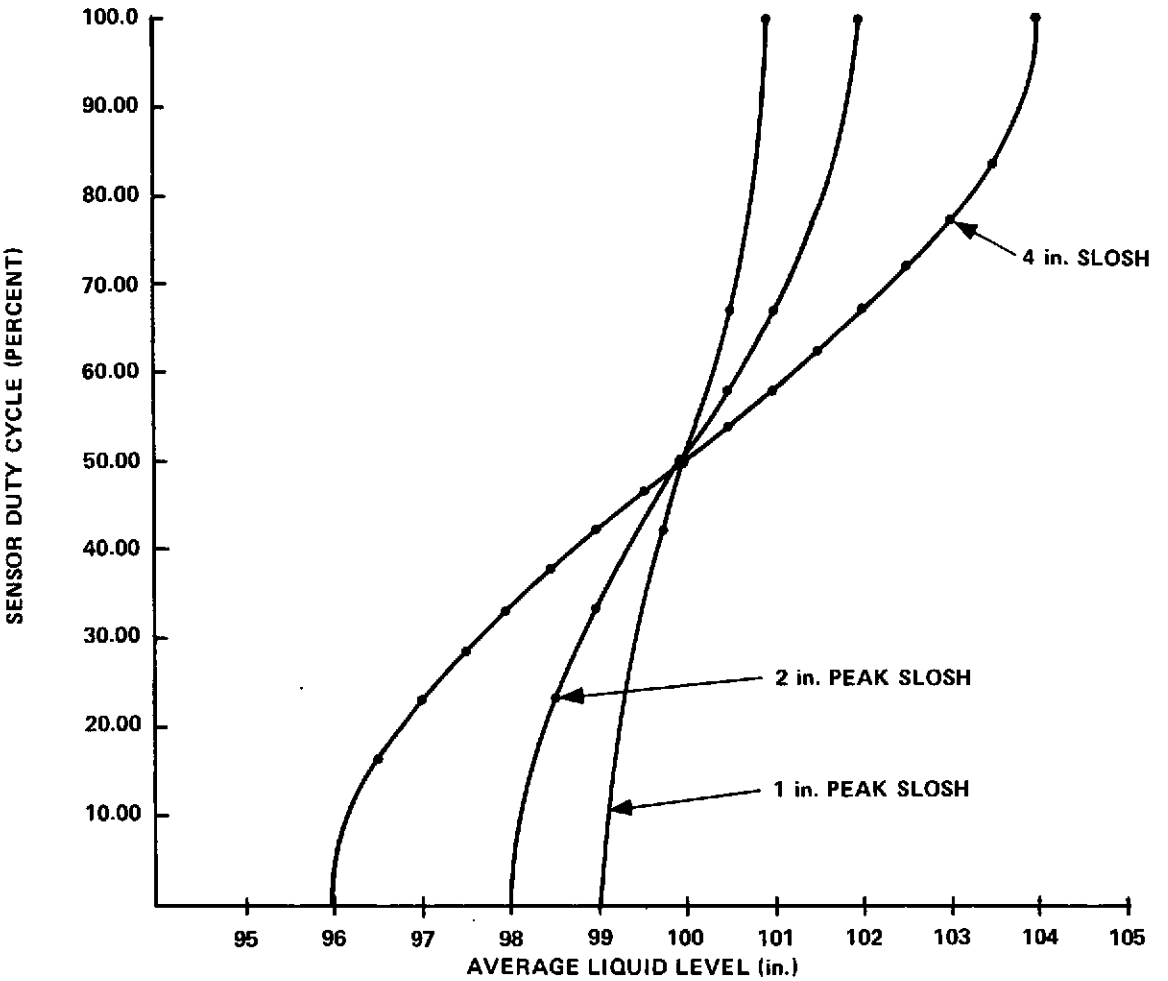

Figure A-1. Point sensor duty cycle versus average liquid level.

APPENDIX B. CONSIDERATION WHEN USING LONG CABLES

In applications requiring long cable lengths between the sensor and signal conditioner, the cable capacitance can be several hundred times larger than the sensor capacitance. Currents will be coupled to the output through this larger capacitance and the cable shield impedance. Current will also be coupled to the output through the sensor shunt capacitances and the cable shield impedance. These currents can be biased out provided they are constant; however, should the cable parameters or sensor shunt capacitances change, or any shield grounding points change impedance, the resulting changing current will cause errors.

Figure B-1 shows the equivalent circuit of the cable and shows how the currents are coupled to the output. R and C represent the cable capacitance and cable shield resistance while C_{ss} represents the sensor shunt capacitance. The dotted line shows a typical error current path. The phase and magnitude of the error currents will be a function of the cable, sensor, and signal conditioner impedances. If the cable shield impedances are sufficiently low, the errors are negligible.

A problem can be caused when redundant measurements are required and both sensors are connected to the structure ground. Currents will be coupled from the excitation supply of one instrument to the input of the other instrument through the sensor shield impedances. The resulting problems can be avoided by selecting different excitation frequencies for the redundant gages.

Other problems can be caused in extreme cases by the excitation supply not being capable of driving the cable capacitance, causing a reduction in sensitivity. When the excitation frequency is sufficiently close to the resonant frequency of the cable inductance, excitation leakage inductance, and sensor shunt capacitance, offset and sensitivity errors will result when these parameters change. These problems can be minimized by appropriate excitation supply design and frequency selection.

Computer programs have been generated to analyze all of the above effects of cables.

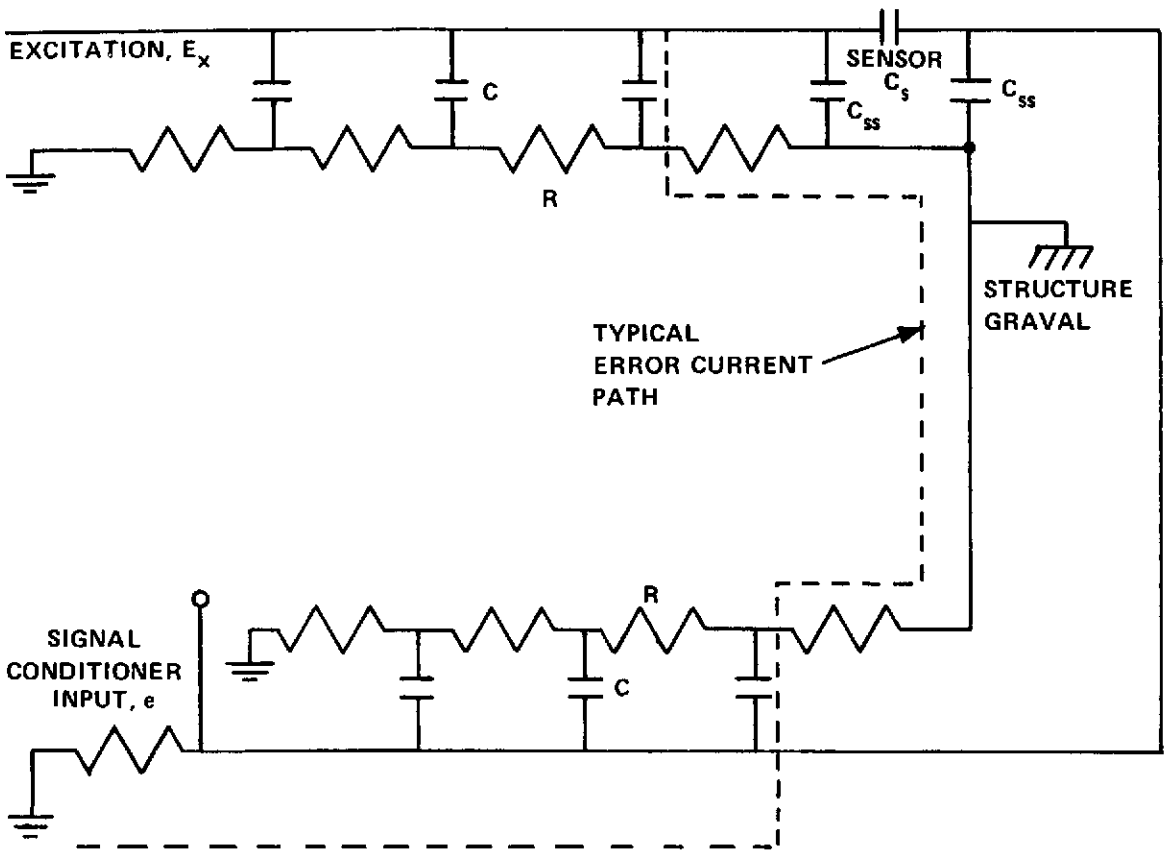

Figure B-1. Equivalent circuit for long cable application.

APPROVAL

SHUTTLE PROPELLANT LOADING INSTRUMENTATION DEVELOPMENT

By John Hamlet

The information in this report has been reviewed for security classification. Review of any information concerning Department of Defense or Atomic Energy Commission programs has been made by the MSFC Security Classification Officer. This report, in its entirety, has been determined to be unclassified.

This document has also been reviewed and approved for technical accuracy.

W. T. ESCUE
Chief, Measuring Sensors Branch

J. L. MACK
Chief, Guidance and Control Division

F. BROOKS MOORE
Director, Electronics and Control Laboratory

☆U.S. GOVERMENT PRINTING OFFICE 1975—640-452/238 REGION NO. 4

DISTRIBUTION

INTERNAL

DA01

SA31
Mr. Odom

AT01

CC01

EA01
Mr. Smith
Dr. Haeussermann

EE01
Mr. Kingsbury

EE31
Mr. Mulloy
Mr. Guzinsky

EC01
Mr. Moore

EC21
Mr. Mack

EC23
Mr. Escue
Mr. Hamlet (10)

EP01
Mr. McCool

EP43
Mr. Worlund

EL42
Mr. Cobb

EL24
Mr. Patterson

ET01
Mr. Reinartz

AS61 (2)

AS61L (8)

EXTERNAL

Scientific & Technical Information
Facility (25)
P.O. Box 33
College Park, Maryland 20740
Attn: NASA Representative (S-AK/RKT)